Supplemental Text:

Results:

(1) MFH-MSC relation: To independently establish the relationship between MFH and MSCs, we isolated total cellular RNA from hMSCs before (day 0) and at days 7, 14, and 21 days after continual growth in the presence of adipogenesis differentiation medium (ADM) as well as at days 7, 14, and 21 in the presence of osteogenesis differentiation medium (ODM). Gene expression profiling of total cellular RNA at these time points was performed on Affymetrix U133a in conjunction with our Genomic Core Facility. Confirmation of progression of differentiation at early time points was confirmed by demonstrating rapid changes in global gene expression via sample similarity comparison to hMSCs via GeneSpring (as compared to hMSCs maintained in cell culture but not induced to differentiate) as well as terminal maturation as seen by cessation of proliferation (data not shown) and acquisition of the mature phenotype (either fat or bone) as determined via fat accumulation as stained with Oil-Red-O or calcium-matrix formation as stained with Aliarin-Red-S (Supplemental Figure 1A, left). Using gene-expression profiles from the differentiating samples, we performed ANOVA (parametric test, variances assumed equal (ANOVA) p-value cutoff 0.05, multiple testing correction: Benjamini and Hochberg False Discovery Rate) on both the differentiating adipocyte and osteogenic series and identified genes that specifically change with adipocytic and osteogenic differentiation time course (Supplemental Table 3 and 4, respectively). Additionally, we also isolated total cellular RNA from both an MFH cell line and a liposarcoma cell line (MFH0022 and LS141, respectively, both generated from human tissue), as well as the SAOS2 osteosarcoma cell line (obtained via ATCC). Using the

complete U133A gene set no association is seen between either cell line and their corresponding lineage (Supplemental Figure 1B, C left panels). However, performing hierarchical clustering using the adipocytic-specific gene set demonstrated that in the adipocytic series, the MFH22 cell line associates with hMSCs, while the LS141 cell line associates with later time points (i.e., cells committed to the adipocytic lineage) (Supplemental Figure 1B, right panel). Similarly, performing hierarchical clustering using the osteogenic gene set demonstrated that in the osteogenic series, the MFH22 cell also associates with the hMSCs, while the SAOS2 cell line associates with later time points (i.e., cells committed to the osteogenic lineage) (Supplemental Figure 1C). This set of differentiation experiments in cell lines independently confirms the association studies described on the human sarcoma samples above.

(2) Genes overexpressed in specific sarcoma sub-types are (not-unexpectedly) representative of the cell/lineage of origin of that particular sub-type: For example, ANOVA on the gene expression profiles of the panel of soft tissue sarcomas described above stratified by genes overexpressed in liposarcomas identifies: lipoprotein lipase (LPL), retinol adipocyte C1Q collagen domain containing (ACDC), glycerol-3-phosphate dehydrogenase 1 (GPD1), fatty acid translocase (CD36), fatty acid binding protein 4 (FABP4), perilipin (PLIN), and peroxisome proliferators activated receptor gamma (PPARG) as eight of the ten most overexpressed genes; all of which are very relevant to adipogenesis and/or adipocytic function. Similarly, ANOVA on gene expression profiles of the panel of soft tissue sarcomas stratified by genes overexpressed in leiomyosarcomas identifies: leiomodin 1 (LMOD1), myosin-heavy chain 11 (MYH11), phospholamban

(PLN), desmin (DES), calponin 1 (CNN1), actin-gamma-2 smooth muscle (ACTG2), myosin light chain kinase (MYLK) as seven of the ten most overexpressed genes; all of which are very relevant to myogenesis or muscle function. These observations provided the rationale for seeking MSC relevant genes in the set of genes identified via ANOVA from gene expression profiles of the panel of soft tissue sarcomas stratified by genes overexpressed in MFH. Please see main text.

(3) Mechanism of β-catenin failure to accumulate in the nucleus: Our data suggests that the reason MFH cells fail to accumulate nuclear β-catenin is due to limited endogenous production; as fitting a hMSC 'transformed' at day 8 of proliferation where endogenous hMSC β-catenin are naturally low (Figure 2E). To validate this possibility we cultured MFH cells in the presence and absence of a polyclonal antibody to DKK1 (PoAb-Dkk1, capable of sequestering DKK1 in the serum, 1ug/ml) as well as with lithium (an activator of β-catenin via inhibition of the Wnt-pathway intermediate inhibitor GSK-3β, 20mM [1]) and assessed for nuclear β-catenin accumulation. Treatment of MFH cells independently with either Lithium or PoAb-Dkk1 results in increased accumulation of total cellular (Supplemental Figure 2A; bottom panel, lanes 4,6); but not nuclear β-catenin accumulation (Supplemental Figure 2A; bottom panel, lanes 4,6). However, treatment of MFH cells concurrently with Lithium and PoAb-Dkk1 results in increased accumulation of total cellular (Supplemental Figure 2A; bottom panel, right-most lane) and nuclear β-catenin accumulation (Supplemental Figure 2A; bottom panel, right-most lane).

To further verify the results obtained in Figure 2A; we chose an siRNA based approach. As a first step, we treated MFH cells with siRNA-DKK1; and stationary/confluent hMSCs with siRNA-Wnt2 and separately siRNA-Wnt5a. Since DKK1, Wnt2 and Wnt5a are secreted proteins that interact with cell surface receptors (i.e., Frizzled) to mediate their signaling effect, we tested the ability of each siRNA to reduce the expression of its intended target by comparing levels of the target gene before and after siRNA treatment in both the media as well as the total cellular extracts of the cells via ELISA. The specificity of each siRNA for its target was also verified by examining the expression levels of the other two genes. As could be seen in Supplemental Figure 2B, siRNA-DKK1 was able to dramatically reduce the expression of DKK1 in both the serum and the total cellular extracts of MFH cells; while having no effect on either WNT2 or WNT5a levels in confluent hMSCs (the latter used as controls since WNT2 and WNT5a are at their highest levels; Figure 3B). Similar effect and specificity was observed using siRNA-Wnt2 and siRNA-Wnt5a (Supplemental Figure 2B).

Having established the suitability of siRNA-Dkk1 to effectively and specifically reduce DKK1 levels, we treated MFH cells under the conditions outlined in Figure 2A using siRNA-Dkk1 and measured both the levels and localization of Dkk1. Consistent with those results obtained in Figure 2A, treatment of MFH cells concurrently with lithium and siRNA-Dkk1 resulted in increased accumulation of total cellular (Supplemental Fig 2C; left panel) and nuclear β-catenin accumulation (Supplemental Fig 2C; right panel). Additionally, we demonstrate that (as seen in Figure 2H) MFH cells in which nuclear β-catenin is present (via treatment with either PoAb-Dkk1+Li, siRNA-

Dkk1+Li, or rWnt2; Supplemental Figure 2D) accumulated LEF, and downregulate cyclin D1 and myc; corresponding to the patterns observed in confluent hMSCs.

Finally to determine that it was in fact the active form of β-catenin (i.e., non-phosphorylated) that was accumulating and to better quantitate its accumulation; the ELISA Human Total beta-Catenin DuoSet IC (R&D, DYC1329E) was used with the substitution of anti-Active β-catenin (anti-ABC, clone 8E7 Upstate) as the capture antibody. As can be seen in Supplemental Figure 2E, compared against confluent hMSCs, at which point β-catenin levels are at their highest during the proliferative cycle (Figure 2C,D); MFH cells under all treatment conditions express less β-catenin, except for concurrent treatment with either both lithium and PoAb-Dkk1 or lithium and siRNA-Dkk1.

(4) β-catenin target gene promoter architecture: the primed repressive state. Our observation that a decrease in cyclin D and c-myc levels (Figure 2H) correlated with an increase in β-catenin levels in hMSCs; and vice versa in MFH cells (where nuclear β-catenin is undetectable) in which cyclin D1 and c-myc are expressed in the absence of β-catenin suggested that β-catenin may be repressing these target genes. To examine this possibility β-catenin nucleosomes were isolated (via chromatin immunoprecipitation, ChIP) and assayed via semi-quantitative PCR for the presence of cyclin D and myc promoters. Primers specific for areas containing previously characterized β-catenin DNA binding sequences in both the myc promoter [2] and cyclin D promoter [3] and validated in ChIP assays were used in these experiments.

ChIP using anti-β-catenin antibodies demonstrated that β-catenin associates with the promoters of its target genes (i.e., myc and cyclin D) only as hMSCs reach confluence, represented as time point '0' (Supplemental Figure 3A and B; second panel; hMSC proliferation lanes) and not seen at pre-confluent conditions, represented as time points '-15,-10, -5' corresponding to days of hMSC growth prior to confluence. These results are in agreement with the pattern of nuclear β-catenin observed in Figure 2F. Additionally, we examined the pattern of β-catenin association at the promoter of its target genes during both adipocytic and osteoblastic differentiation. Wnt/β-catenin signaling has been previously shown to be critical for osteoblastic differentiation [4] and inhibitory for adipocytic differentiation [5]. In agreement with these observations we were unable to show a significant association of β-catenin with either the myc promoter or the cyclin D promoter in cells treated with adipocytic differentiation medium (Supplemental Figure 3A and B; second panel; hMSC ADM lanes); while β-catenin was readily detected associating with its target promoters in hMSCs treated with osteoblastic differentiation medium (Supplemental Figure 3A and B; second panel; hMSC ODM lanes). Finally, we examined the relationship between β-catenin and its association with its target genes in MFH cells in which no nuclear β-catenin is detectable (Figure 2F). In agreement with the lack of nuclear β-catenin, no association with its target genes was detectable via ChIP (Supplemental Figure 3A and B; second panel; MFH 'No Tx' lane). As discussed in other parts of this manuscript (Figure 4, Supplemental Figure 2, and Figure 5), recapitulating MSC Wnt-signaling patterns in MFH cells at the point of commitment further allows these MFH-primed cells to be differentiated along adipocytic and osteoblastic lineages (Figure 6A-D). If Wnt-signaling is so crucial to hMSC

commitment to differentiation, and if Wnt/β-catenin has a repressor role on its target genes at the point of commitment, than we theorized that MFH cells in which Wnt/β-catenin signaling is re-established should exhibit similar patterns to hMSCs in terms of β-catenin promoter target associations. MFH cells were treated with either rhWnt2 and rWnt5a or rhWnt2 and rWnt5a followed by further treatment with ADM or ODM. MFH cells treated rhWnt2 and rWnt5a showed that β-catenin was now detectable associating with the myc and cyclin D promoter (Supplemental Figure 3A and B; second panel; MFH 'rhWnt2 and rWnt5a' lanes). This is in agreement with activation of Wnt signaling being able to increase levels of β-catenin leading to nuclear accumulation (Supplementary Figure 2A,C). Further treatment of 'rWnt2 and hWnt5a' MFH cells for 7 days with either ADM or ODM resulted in readily detectable β-catenin association with its target promoters following ODM treatment and no detection in MFH cells treated with ADM (Supplemental Figure 3A and B; second panel; MFH 'rhWnt2 and rWnt5a' lanes +ADM or +ODM). These results are in agreement with those observed in differentiation hMSCs (Supplemental Figure 3A and B; second panel; hMSC ADM or ODM lanes).

Having established that β-catenin binds its target promoters under conditions when it is detectable in the nucleus (as discussed above) we next sought to determine the architectural structure (i.e., open/active or closed/repressed) of myc and cyclin D bound promoters. Although previous data has suggested that β-catenin functions as a transcriptional activator on the myc [6] and cyclin D promoter [7, 8], our data (Figure 2H) suggested that β-catenin was repressing these target genes in mesenchymal cells. Since β-catenin has been previously shown to function as either an activator or repressor on specific genes depending on context (e.g., Sox 9 [9, 10]), the formal analysis of the

promoter architecture of the myc and cyclin D bound β-catenin promoter in mesenchymal cells has not been examined and in light of our observations was a critical point to address. Since our data suggested that β-catenin was repressing myc and cyclin D expression, we sought to detect whether or not the classical 'histone 3 lysine 27 methyl' repressor mark [11] was present, while the classical 'histone 3 lysine 4 methyl' active mark [12]was absent at myc and cyclin D bound β-catenin promoters under the conditions discussed above. As a control we used hMSCs differentiating along the osteoblastic lineage since Wnt/β-catenin is known to be necessary for osteoblastic differentiation (as discussed above) and present at both myc and cyclin D promoter during that process (Supplemental Figure 3A and B; second panel; 'hMSC ODM' lanes). We reasoned that differentiating hMSCs along the osteoblastic lineage should have an active chromatin mark (i.e., histone 3 lysine 4 methyl; H3K4Me) and not show the repressed chromatin mark (histone 3 lysine 27 methyl; H3K27Me). To assess which chromatin modification associated with β-catenin at both the myc and cyclin D promoter, we performed sequential ChIP assays (Re-ChIP) in which β-catenin nucleosomes were selected in the first immunoprecipitation (IP) and after elution from the protein G Sepharose beads were subjected to a second IP with antibodies against either H3K27Me or H3K4Me. IP with an antibody β-catenin followed by IP with an antibody against the active mark H3K4Me in hMSCs differentiating along the osteoblastic lineage showed that the active H3K4Me mark is found in β-catenin immunoprecipitated complexes at both the myc and cyclin D promoters (Supplemental Figure 3A and B; fourth panel; 'hMSC ODM' lanes). On the contrary, IP with an antibody against β-catenin followed by IP with an antibody against the repressive mark H3K27Me in hMSCs differentiating

along the osteoblastic lineage showed that the repressive H3K27Me mark is not found in β-catenin immunoprecipitated complexes at both the myc and cyclin D promoters (Supplemental Figure 3A and B; third panel; 'hMSC ODM' lanes). The absence of the repressive mark and presence of the active mark on β-catenin bound myc and cyclin D promoters during osteoblastic differentiation is in agreement with the osteoblastic promoting role Wnt/β-catenin signaling during osteoblastic differentiation [4].

Similar examination of the status of β-catenin bound myc and cyclin D promoters in confluent hMSCs gave somewhat surprising results. IP with an antibody against β-catenin followed by IP with an antibody against the either repressive mark H3K4Me or H3K27Me in confluent hMSCs showed that both marks are associated with β-catenin bound myc and cyclin D promoters in confluent hMSCs (Supplemental Figure 3A and B; third and fourth panel; 'hMSC '0' lanes; respectively). To examine the issues of whether or not the immunoprecipitated fraction containing β-catenin/H3K27 fraction of β-catenin bound myc and cyclin D promoters was the same or different fraction than the immunoprecipitated fraction containing β-catenin/H3K4 bound myc and cyclin D promoters; we performed sequential ChIP assays (Re-ChIP) in which β-catenin nucleosomes were selected in the first immunoprecipitation (IP) and after elution from the protein G Sepharose beads were subjected to a second IP with antibodies against H3K27Me; and after further elution from the protein G Sepharose beads were subjected to a third IP with antibodies against or H3K4Me. Such sequential IP indicated β-catenin bound myc and cyclin D promoters in confluent hMSCs are simultaneously modified by both the active mark H3K4 and the repressor mark H3K27 (Supplemental Figure 3A and B; fifth panel; 'hMSC '0' lane). Similar results were observed in MFH cells treated with

rWnt2 and rWnt5a , which as shown previously recapitulate hMSC signaling patterns at confluence (Supplemental Figure 3A and B; fifth panel; 'MFH rWnt2 + rWnt5a') lane). Furthermore, MFH cells pre-treated with rWnt2 + rWnt5a behave as hMSC when they are treated with osteogenic differentiation medium (ODM) loosing the repressive H3K27 mark and expressing only the active H3K4 mark (Supplemental Figure 3A and B; comparing fourth and fifth panels). Thus our data indicates that the simultaneous active and repressive mark of β-catenin bound myc and cyclin D promoters exists only in confluent hMSCs and MFH cells in which Wnt signaling of confluent hMSCs is recapitulated.

Although our semi-quantitative PCR data indicated that there was approximately the same amount of β-catenin/H3K4/H3K27 complexes as there were β-catenin/H3K4 and β-catenin/H3K27 complexes suggesting that all β-catenin bound myc and cyclin D promoter complexes in hMSCs at confluence and MFH cells treated with rWnt2 and rWnt5a were simultaneously modified with both the active and repressed mark (Supplemental Figure 3A and B; hMSC '0' and 'MFH rWnt2 and rWnt5a' lanes), we additionally performed quantitative PCR using the SYBR GreenER Quantitative PCR Kit (Invitrogen) with Rox as a reference dye to objectively analyze our results. First thermal dissociation curves using serial 10-fold dilutions of input genomic DNA (i.e., no antibody IP control) were used to establish a standard curve (Supplemental Figure 4 A, B; blue squares and diagonal blue line as best fit model). Each serial dilution standard curve was performed three times starting each time with individually recovered genomic DNA following no antibody IP. Thus each time point analyzed had three replicates. Averages of normalized values are shown as blue squares. Thermal dissociation curves (of a

representative standard dilution series) as an indicator of primer specificity across the given DNA input range are shown in the upper inset of each curve. Sample thermal dissociation curves corresponding to ChIP product of total input (A,F), hMSC- β-catenin (B,G), hMSC- β-catenin/H3K27 (C,H), hMSC- β-catenin/H3K4 (D,I), and hMSC- β-catenin/H3K27H3K4 (E,J) for either hMSCs at confluence (Supplementary Figure 4a; samples A-E) or MDF cells treated with rWnt2 and rWnt5a (Supplementary Figure 4a; samples F-J) corresponding to PCR products shown in Supplementary Figure 3 are also shown in right upper insets as an indicator or PCR specificity under the given input conditions. As for the standards, each IP represents the averaged normalized values of three replicates. As could be seen for both β-catenin bound myc and cyclin D promoter complexes in hMSCs at confluence and MFH cells treated with rWnt2 and rWnt5a, in the absence of an immunoprecipitating antibody (Supplemental Figure 3A,B; samples A,F), total quantity PCR product approximates identical quantity used for generation of first PCR standard. Further the subsequent tight grouping of samples B-E or G-J corresponding to immunoprecipitation products with β-catenin and then sub-sequent single or bivalent chromatin modifications for either hMSCs (B-E) or MFH (G-J) under the indicated conditions, suggests that β-catenin/H3K27H3K4 account for the majority of β-catenin bound myc and cyclin D promoters. Although, the samples due to show tight grouping on a logarithmic scale, and would appear all to be within one log of each other, there is a noticeable decline as samples proceed from the first IP (β-catenin alone), to the second, (β-catenin/H3K27 or β-cateni/H3K4) to the third (β-catenin/H3K27). It is entirely possible that β-catenin/H3K27/H3K4 complexes do not account for all the complexes and that some, although it would have a minor amount in comparison, of

either unmodified or singly modified β-catenin complexes at myc and cyclin D promoters exist under the indicated conditions. Alternatively, a reasonable explanation might be the decreased efficiency and product recovery with each subsequent immunoprecipitation.

The presence of a simultaneous active and repressive histone marks has been previously reported and termed “bivalent chromatin” domains [13]. These domains have been reported to mark genes that are critical to cell/tissue specification in embryonic stem cells [13]. These bivalent chromatin modifications are believed to identify genes 'poised' or kept in a repressed but readily activatable state [14]; in essence priming those genes for activity. Although, bivalent chromatin structures of β-catenin bound myc and cyclin D promoters have not previously been reported to the best of our knowledge; embryonic specific gene (e.g., Oct4, nanog; [13]), tissue specific transcription factors (e.g., Gata-4,5; [15]), and general cell cycle regulators (e.g., p16; [15]) have all been reported to possess bivalent chromatin structures in specific situations. Given the importance, as presented here, and the plethora of articles citing the importance (either positive or negative) to Wnt/β-catenin signaling in mesenchymal development, it may not be surprising that β-catenin target genes exhibit bivalent chromatin architecture at the point where the decision to commit to a specific lineage is made. Clearly more work is necessary to accurately define the role of β-catenin target gene promoter bivalent chromatin domains in MSCs.

(5) Expression of ‘early markers of mesenchymal differentiation’ (EMofMD) using lithium and polyclonal antibodies against DKK1. Since 1) cessation of proliferation as a function of confluence is a prerequisite for MSC in vitro differentiation [1, 16]; 2) β-

catenin accumulates in the nucleus during that process (Figure 2D); 3) DKK1 has been shown to promote MSC proliferation and interfere with differentiation [1]; and 4) our recent evidence that MFH may represent a transformed hMSC – we further hypothesized that our ability to induce nuclear β-catenin in MFH cells may be sufficient to prime the cells for mesenchymal differentiation. Since normal hMSC terminal differentiation requires three-four weeks of culturing and markers of terminal differentiation are observed only in the latter week of growth, and since it is possible that MFH cells may only be partially differentiable (i.e., they may commit but not complete terminal differentiation) if at all, we sought to determine "early" markers of mesenchymal differentiation (EMofMD) that might be expressed by MFH rapidly if they are able to commit to mesenchymal differentiation. To determine EMofMD we overlapped the following four lists of genes: genes absent in MSCs, genes absent in MFH, genes present in hMSCs three days after treatment with either ADM or ODM. This approach is diagrammed in Supplemental Figure 3A. Presence and absence were determined via GeneSpring Software of raw gene expression data. The rationale was that if genes not present in hMSCs but upregulated in hMSCs after treatment with either ADM or ODM, were similarly absent in MFH and upregulated with treatment, this might be an early indication that MFH cells were committing to the differentiation program. 10 transcripts representing 7 genes were identified; four genes (CRLF1, DLX5, FKBP1B, WFDC1) were chosen for confirmation via RT-PCR. To confirm GeneSpring gene expression analysis, expression of these four genes, from this point referred to as early markers of mesenchymal differentiation – EMofMD, in MFH was assessed via RT-PCR on RNA extracted from a panel of soft-tissue sarcomas. In agreement with gene expression

analysis no expression of these four genes was detectable in MFH tissue (Supplemental Figure 3B, left panel). Similarly, no expression of these four genes was detected via RT-PCR analysis performed on RNA isolated from undifferentiated hMSCs (A0, B0; Supplemental Figure 3B, mid, right panel). However, rapid accumulation of all four genes was observed via RT-PCR analysis on RNA isolated from time points during both adipocytic and osteogenic differentiation (Supplemental Figure 3B, mid, right panel).

Having identified a group of genes representative of early differentiation we next sought to examine whether these genes are upregulated in MFH cells after treatment with either ADM or ODM and in the presence or absence of β-catenin. MFH cells were treated for 24 hours with lithium and PoAb-DKK1 (as well as multiple controls) and then further cultured in the presence of either ADM or ODM. RNA was extracted after three days of culturing and RT-PCR was performed for EMofMD (Supplemental Figure 3C). The EMofMD were observed only in hMSCs treated with ADM or ODM (positive control; Supplemental Figure 3C, lane A) and only in MFH cells pre-treated with the combination of lithium and PoAb-DKK1 (Supplemental Figure 3C; lane J). Note that this treatment corresponds with nuclear β-catenin accumulation in MFH cells (Supplemental Figure 2A; right-most lane). This data taken together suggests that 1) the combination of lithium and PoAb-Dkk1 is necessary for β-catenin nuclear accumulation in MFH cells; and 2) specific pre-treatment of MFH cells with this combination in the presence of differentiation media results in commitment of MFH cells to differentiation as assayed via EMofMD.

Materials and Methods:

hMSC – Cell Culture and Differentiation.

hMSCs were kindly provided by Darwin Prockop of Tulane University and propagated in continuous culture medium (CCM: 20% FBS, Atlanta Bio in DMEM, GibcoBRL). Adipogenesis was accomplished by continuous culturing in adipogenic differentiation medium (ADM) containing CCM supplemented with 20 0.5uM dexamethasone, 0.5uM isobutylmethylxanthine, and 50uM indomethacin for 21 days. Osteogenesis was accomplished by continuous culturing in osteogenic differentiation medium (ODM) containing CCM supplemented with 10-8 M dexamethasone, 5mM β-glycerophosphate, and 50ug/ml L-ascorbic acid for 21 days. Oil-Red-O (Sigma) and Alizarin-Red-S (Sigma) staining were performed as previously described [16].

RNA Isolation, RT-PCR, Primers:

Total cellular RNA was isolated from proliferating hMSCs and MFH0022 (treated and/or untreated as indicated in the text) at the indicated time points using RNeasy kits from Qiagen (Valencia, CA). Total cellular RNA was hybridized on U133a Affymetrix array by MKSCC Genomic Core Facility. SuperScript One-Step RT-PCR with Platinum Taq (GIBCO BRL Life Technologies, Gaithersburg, MD) was used on 2ul of total cellular RNA and cDNA synthesis was performed at 55°C for 30 min, and PCR amplification consisted of initial denaturing at 94°C, followed by 40 cycles of 15 sec at 94°C, 30 sec at

the adequate annealing temperature according to each primer couple and 40 sec at 72°C. Annealing temperatures ranged from 55° to 65°C. Primers were designed via Primer3:

DKK-1=5-CATATGGCCGCGTTGATGCGGAGCAAGGAT-3 & 5-CCTAGGTCAAATTTTCTGACACACATGGAG–3;

GADPH = 5-CCCCTTCATTGACCTCAACT-3 & 5-CGACCGTAACGGGAGTTGCT-3;

FKBP1B=5-GTGGATCCGCTATGGGCGTGGAGAT-3 & 5-AAGGATCCGTCCCAGTGGCAGAGCAG-3;

DLX5=5-5-TGGCAAACCAAAGAAAGTTC-3 and 5-AATAGAGTGTCCCGGAGG-3;

CRLF1=5'- GCAGAGGGAAGAGGAGGAAAACAGA-3 & CACACCACTATGCGACAGAATGAG-3.

All fresh frozen sarcoma samples were obtained via MSKCC Department of Pathology Tumor Bank via IRB 02-020.

ChIP:

Chromatin immunoprecipitation (ChIP) and sequential ChIP assays were performed as previously described ([17, 18]). Myc promoter primers [2]: 5′-ACCTCGACTACGACTCGGTG-3′ and 5′-AGAAGCCGCTCCACATACAG-3′. Cyclin D promoter [3] 5'-GCTTTCCATTCAGAGGTGTG-3' and 5'-CCGAAAATTCCAGCAGCAGC-3'. IP antibodies: Anti-β-Catenin (BD BioSciences Transduction Laboratories 610154); anti-H3K4Me2 antibody (Upstate; 07-030); anti-H3K27Me2 antibody (Cell Singaling #9755).

Quantitative PCR:

Quantitative PCR was performed using the SYBR GreenER Quantitative PCR Kit (Invitrogen) with Rox as a reference dye per the manufacturer's instructions on the Stratagene Mx3005P Unit. Data was analyzed using the Stratagene MxPro Software Package. Myc promoter primers and cyclin D promoters were used as for ChIP (above).

ELISA:

DKK1, Wnt2, and Wnt 5a levels were measured via the ELISA Human Total β-catenin DuoSet IC (R&D, DYC1329E) per the manufacturers guidelines, except for the substitution of human Dkk1 (R&D Human Affinity Purified Polyclonal Ab, AF1096); Wnt2 (Santa Cruz H-20, SC5208); or Wnt5a (Santa Cruz H-58, SC30244); respectively as the capture antibody after appropriate titrations.

REFERENCES:

1. Gregory, C.A., et al., *Dkk-1-derived synthetic peptides and lithium chloride for the control and recovery of adult stem cells from bone marrow.* J Biol Chem, 2005. **280**(3): p. 2309-23.
2. Rodriguez, J.L., et al., *Id2 leaves the chromatin of the E2F4-p130-controlled c-myc promoter during hepatocyte priming for liver regeneration.* Biochem J, 2006. **398**(3): p. 431-7.
3. Toualbi, K., et al., *Physical and functional cooperation between AP-1 and beta-catenin for the regulation of TCF-dependent genes.* Oncogene, 2007. **26**(24): p. 3492-502.
4. Krishnan, V., H.U. Bryant, and O.A. Macdougald, *Regulation of bone mass by Wnt signaling.* J Clin Invest, 2006. **116**(5): p. 1202-9.
5. Ross, S.E., et al., *Inhibition of adipogenesis by Wnt signaling.* Science, 2000. **289**(5481): p. 950-3.
6. He, T.C., et al., *Identification of c-MYC as a target of the APC pathway.* Science, 1998. **281**(5382): p. 1509-12.
7. Tetsu, O. and F. McCormick, *Beta-catenin regulates expression of cyclin D1 in colon carcinoma cells.* Nature, 1999. **398**(6726): p. 422-6.
8. Shtutman, M., et al., *The cyclin D1 gene is a target of the beta-catenin/LEF-1 pathway.* Proc Natl Acad Sci U S A, 1999. **96**(10): p. 5522-7.
9. Blache, P., et al., *SOX9 is an intestine crypt transcription factor, is regulated by the Wnt pathway, and represses the CDX2 and MUC2 genes.* J Cell Biol, 2004. **166**(1): p. 37-47.
10. Hill, T.P., et al., *Canonical Wnt/beta-catenin signaling prevents osteoblasts from differentiating into chondrocytes.* Dev Cell, 2005. **8**(5): p. 727-38.
11. Kirmizis, A., et al., *Silencing of human polycomb target genes is associated with methylation of histone H3 Lys 27.* Genes Dev, 2004. **18**(13): p. 1592-605.
12. Bernstein, B.E., et al., *Genomic maps and comparative analysis of histone modifications in human and mouse.* Cell, 2005. **120**(2): p. 169-81.
13. Bernstein, B.E., et al., *A bivalent chromatin structure marks key developmental genes in embryonic stem cells.* Cell, 2006. **125**(2): p. 315-26.
14. Spivakov, M. and A.G. Fisher, *Epigenetic signatures of stem-cell identity.* Nat Rev Genet, 2007. **8**(4): p. 263-71.
15. Ohm, J.E., et al., *A stem cell-like chromatin pattern may predispose tumor suppressor genes to DNA hypermethylation and heritable silencing.* Nat Genet, 2007. **39**(2): p. 237-42.
16. Gregory, C.A., et al., *The Wnt signaling inhibitor dickkopf-1 is required for reentry into the cell cycle of human adult stem cells from bone marrow.* J Biol Chem, 2003. **278**(30): p. 28067-78.
17. Kouskouti, A. and I. Talianidis, *Histone modifications defining active genes persist after transcriptional and mitotic inactivation.* Embo J, 2005. **24**(2): p. 347-57.

18. Rekhtman, N., et al., *PU.1 and pRB interact and cooperate to repress GATA-1 and block erythroid differentiation.* Mol Cell Biol, 2003. **23**(21): p. 7460-74.

Supplemental Figure Legends:

Supplemental Figure 1: Differentiation of hMSCs into connective tissue lineages: (A) hMSCs staining with hematoxylin and eosin (top left), hMSCs after 21 days culturing in adipogenesis medium stained with Oil-Red-O (bottom left), hMSCs after 21 days culturing with osteogenesis medium stained with Alizarin-Red-S. Percent similarity based on global gene expression profile as a function of the undifferentiated state (right panel). (B) Unsupervised hierarchical clustering of a panel of soft tissue sarcomas (described in detail [9]) using full U133A gene array (left panel) using genes differentially expressed during the adipogenesis differentiation time course (Supplemental Table 3). (C) Unsupervised hierarchical clustering of a panel of soft tissue sarcomas (described in detail [9]) using full U133A gene array (left panel) using genes differentially expressed during the osteogenic differentiation time course (Supplemental Table 4).

Supplemental Figure 2: Nuclear localization of β-catenin in MFH. (A) Immunoblot analysis of β-catenin in total, nuclear, and cytoplasmic extracts in the indicated cells following the indicated treatments. (B) ELISA of DKK1 in MFH cells, and WNT2, and WNT5a in stationary hMSCs before and after treatment with the corresponding antibody or siRNA. Please see main text, Materials and Methods, for details. (C) Immunoblot analysis of β-catenin in total, nuclear, and cytoplasmic extracts in the indicated cells following the indicated treatments. (D) Immunoblot analysis of the indicated proteins in

MFH cells following indicated treatment conditions. (E) ELISA quantitation of β-catenin activity in total cellular extracts from (A) and (B) and (C).

Supplemental Figure 3: Chromatin immunoprecipitation of β-catenin bound myc (A) and cyclin D (B) promoters under the indicated immunoprecipitation conditions in the indicated cells. Please see text for details.

Supplemental Figure 4: Quantitative PCR of β-catenin bound myc (A) and cyclin D (B) promoters under the indicated immunoprecipitation conditions in the indicated cells. Please see text for details.

Supplemental Figure 5: Identification of early markers of mesenchymal differentiation (EMoMD). (A) Schematic representation of gene lists overlapped to identify EMoMD. (B) RT-PCR of EMoMD in indicated sarcomas and during adipocytic and osteogenic differentiation. (C) Expression of EMoMD via RT-PCR in the indicated cells treated under identical conditions as in Supplemental Figure 2A.

Supplemental Figure 6: Schematic representation of the relationship between hMSCs and MFH cells focusing on the role Wnt signaling as a crucial mediator between the two states. Please see main and supplemental text for details.

Supp Fig 1:

A.

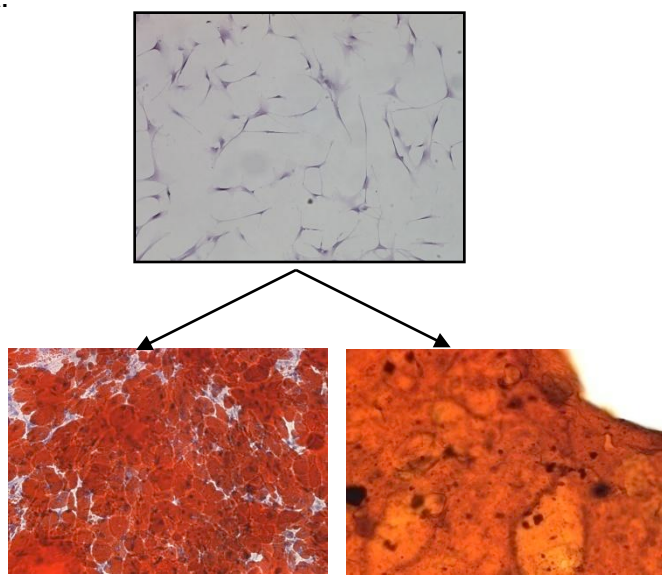

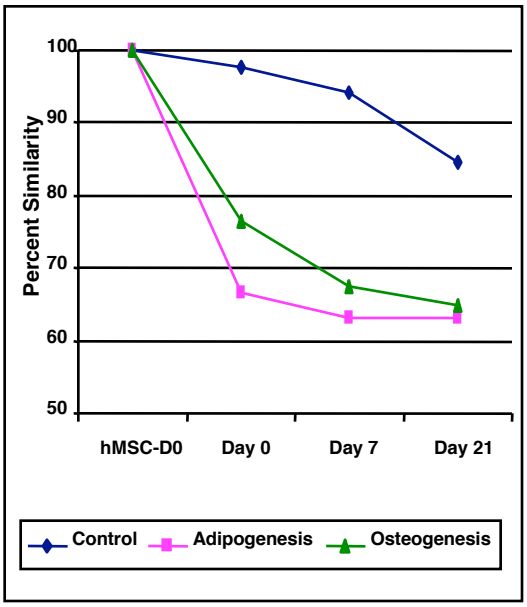

B.

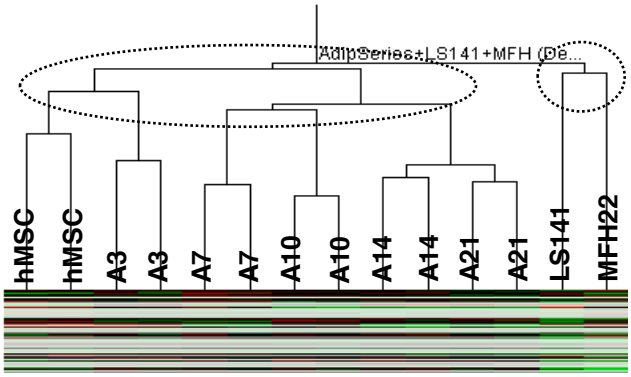

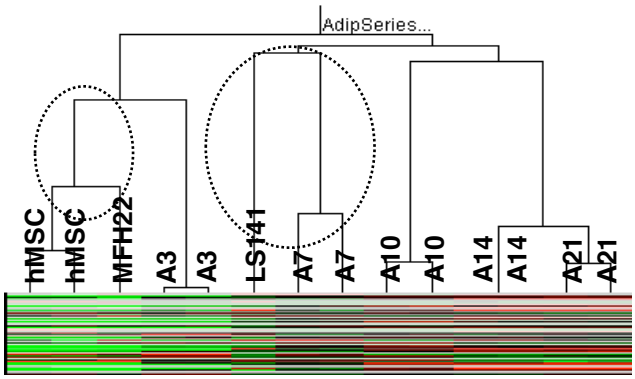

C.

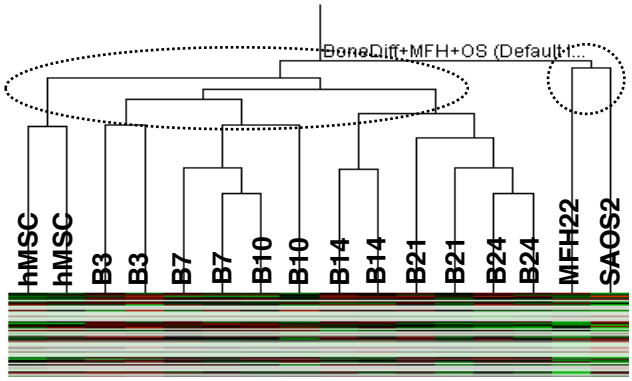

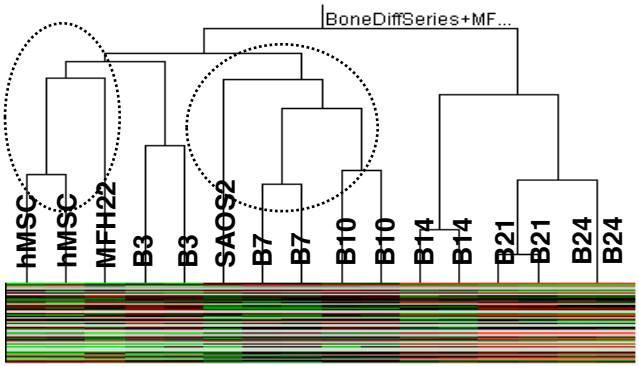

Supp Fig 2:

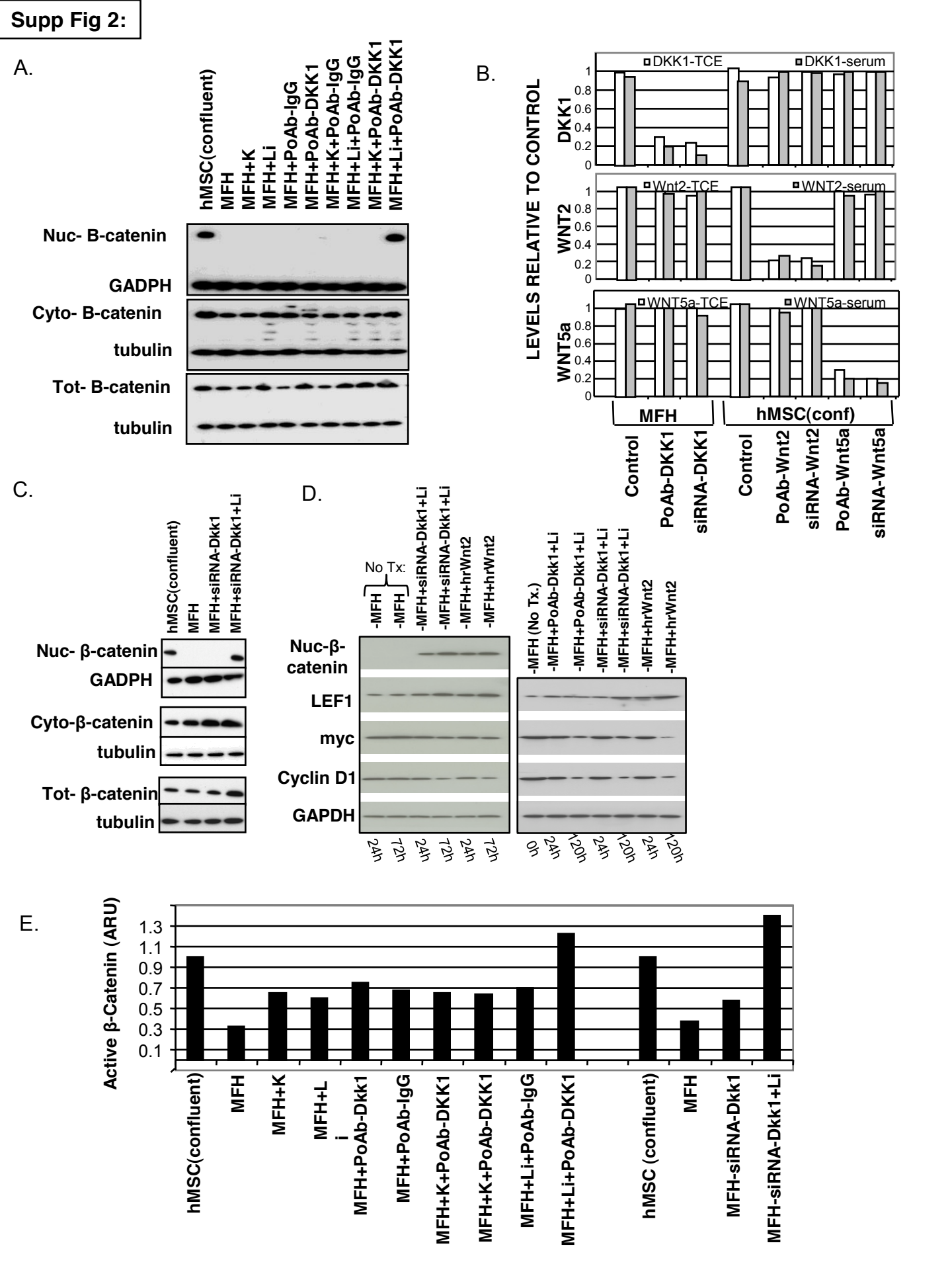
A.
hMSC(confluent)
MFH
MFH+K
MFH+Li
MFH+PoAb-IgG
MFH+PoAb-DKK1
MFH+K+PoAb-IgG
MFH+Li+PoAb-IgG
MFH+K+PoAb-DKK1
MFH+Li+PoAb-DKK1
Nuc- B-catenin
GADPH
Cyto- B-catenin
tubulin
Tot- B-catenin
tubulin
B.
LEVELS RELATIVE TO CONTROL
DKK1
DKK1-TCE
DKK1-serum
WNT2
Wnt2-TCE
WNT2-serum
WNT5a
WNT5a-TCE
WNT5a-serum
MFH
hMSC(conf)
Control
PoAb-DKK1
siRNA-DKK1
Control
PoAb-Wnt2
siRNA-Wnt2
PoAb-Wnt5a
siRNA-Wnt5a
C.
hMSC(confluent)
MFH
MFH+siRNA-Dkk1
MFH+siRNA-Dkk1+Li
Nuc- β-catenin
GADPH
Cyto-β-catenin
tubulin
Tot- β-catenin
tubulin
D.
No Tx:
-MFH
-MFH
-MFH+siRNA-Dkk1+Li
-MFH+siRNA-Dkk1+Li
-MFH+hrWnt2
-MFH+hrWnt2
Nuc-β-catenin
LEF1
myc
Cyclin D1
GAPDH
24h
72h
24h
72h
24h
72h
-MFH (No Tx.)
-MFH+PoAb-Dkk1+Li
-MFH+PoAb-Dkk1+Li
-MFH+siRNA-Dkk1+Li
-MFH+siRNA-Dkk1+Li
-MFH+hrWnt2
-MFH+hrWnt2
0h
24h
120h
24h
120h
24h
120h
E.
Active β-Catenin (ARU)
1.3
1.1
0.9
0.7
0.5
0.3
0.1
hMSC(confluent)
MFH
MFH+K
MFH+L
i
MFH+PoAb-Dkk1
MFH+PoAb-IgG
MFH+K+PoAb-DKK1
MFH+K+PoAb-DKK1
MFH+Li+PoAb-IgG
MFH+Li+PoAb-DKK1
hMSC (confluent)
MFH
MFH-siRNA-Dkk1
MFH-siRNA-Dkk1+Li

Supp Fig 3:

A.

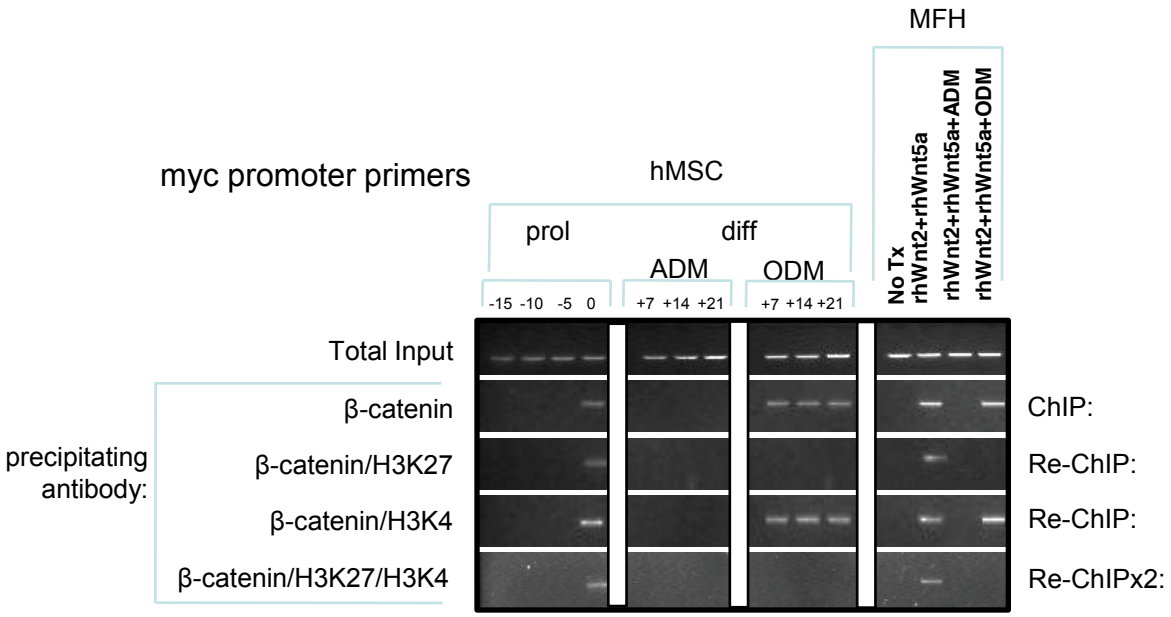
myc promoter primers
hMSC
prol
diff
ADM
ODM
-15 -10 -5 0
+7 +14 +21
+7 +14 +21
MFH
No Tx
rhWnt2+rhWnt5a
rhWnt2+rhWnt5a+ADM
rhWnt2+rhWnt5a+ODM
Total Input
β-catenin
β-catenin/H3K27
β-catenin/H3K4
β-catenin/H3K27/H3K4
precipitating antibody:
ChIP:
Re-ChIP:
Re-ChIP:
Re-ChIPx2:

B.

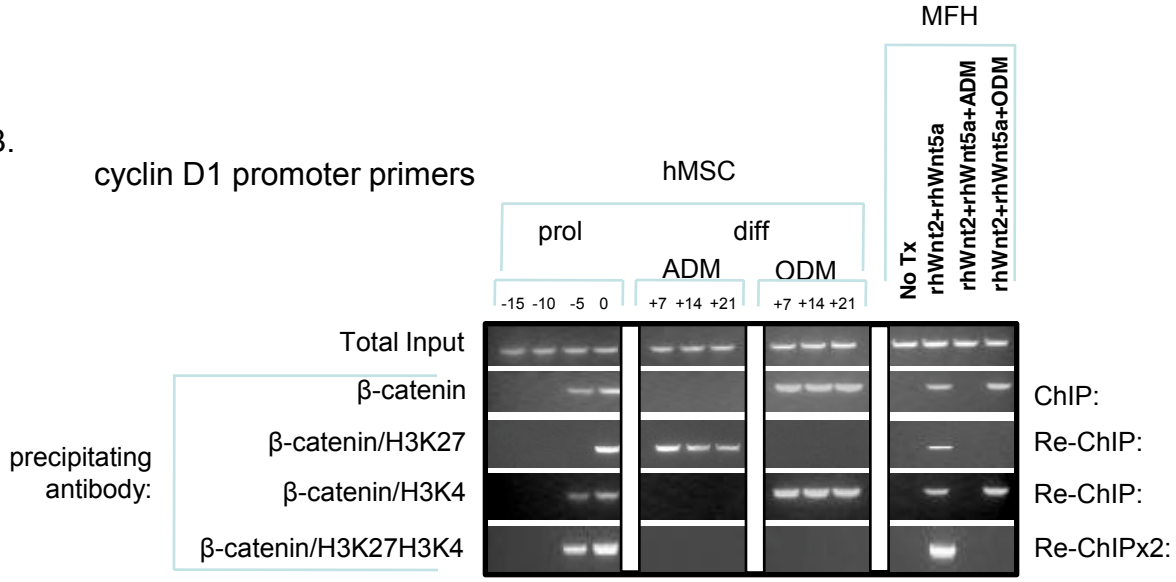
cyclin D1 promoter primers
hMSC
prol
diff
ADM
ODM
-15 -10 -5 0
+7 +14 +21
+7 +14 +21
MFH
No Tx
rhWnt2+rhWnt5a
rhWnt2+rhWnt5a+ADM
rhWnt2+rhWnt5a+ODM
Total Input
β-catenin
β-catenin/H3K27
β-catenin/H3K4
β-catenin/H3K27H3K4
precipitating antibody:
ChIP:
Re-ChIP:
Re-ChIP:
Re-ChIPx2:

Supp Fig 4:

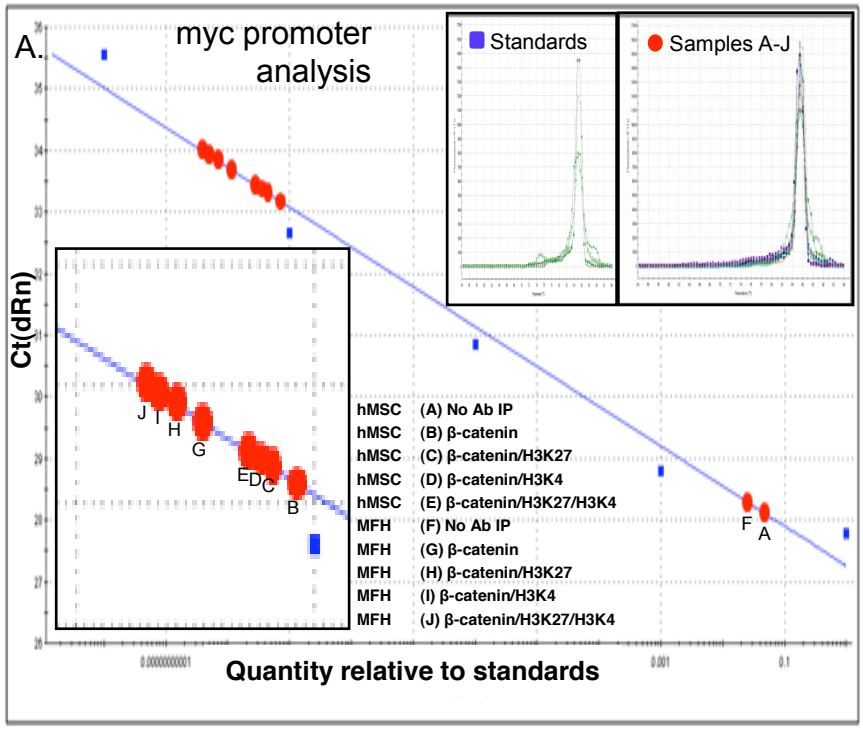
A.
myc promoter analysis
Standards
Samples A-J
Ct(dRn)
J
I
H
G
E
D
C
B
F
A
hMSC (A) No Ab IP
hMSC (B) β-catenin
hMSC (C) β-catenin/H3K27
hMSC (D) β-catenin/H3K4
hMSC (E) β-catenin/H3K27/H3K4
MFH (F) No Ab IP
MFH (G) β-catenin
MFH (H) β-catenin/H3K27
MFH (I) β-catenin/H3K4
MFH (J) β-catenin/H3K27/H3K4
Quantity relative to standards

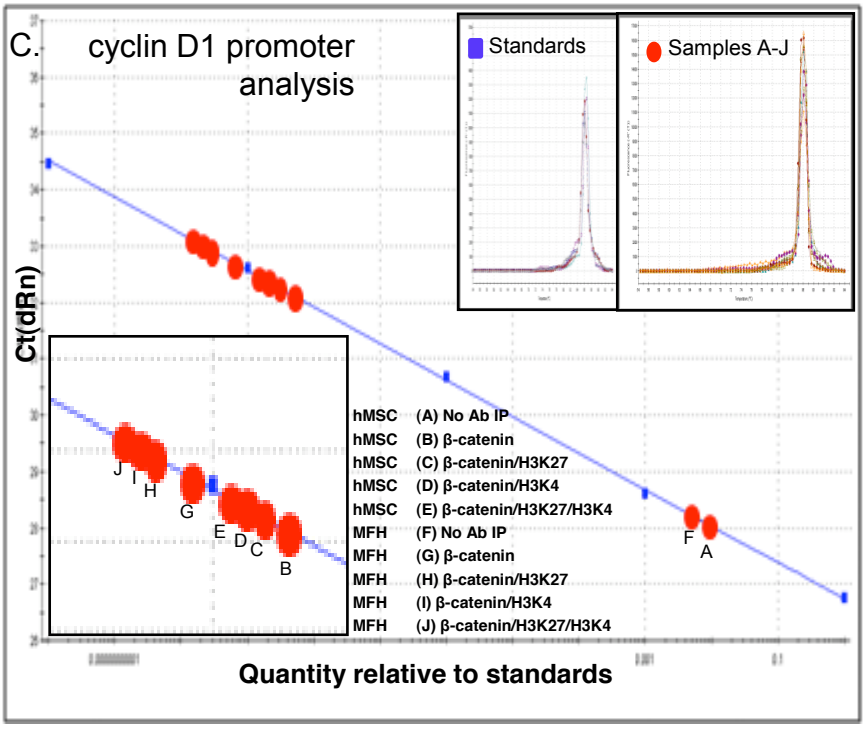
C.
cyclin D1 promoter analysis
Standards
Samples A-J
Ct(dRn)
J
I
H
G
E
D
C
B
F
A
hMSC (A) No Ab IP
hMSC (B) β-catenin
hMSC (C) β-catenin/H3K27
hMSC (D) β-catenin/H3K4
hMSC (E) β-catenin/H3K27/H3K4
MFH (F) No Ab IP
MFH (G) β-catenin
MFH (H) β-catenin/H3K27
MFH (I) β-catenin/H3K4
MFH (J) β-catenin/H3K27/H3K4
Quantity relative to standards

Supp Fig 5:

A.

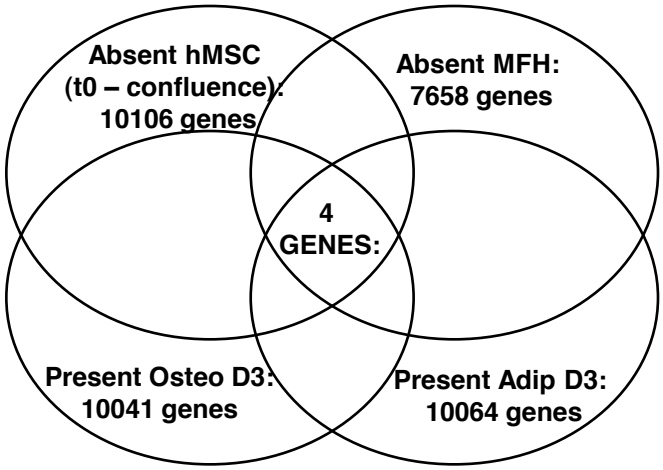

B.

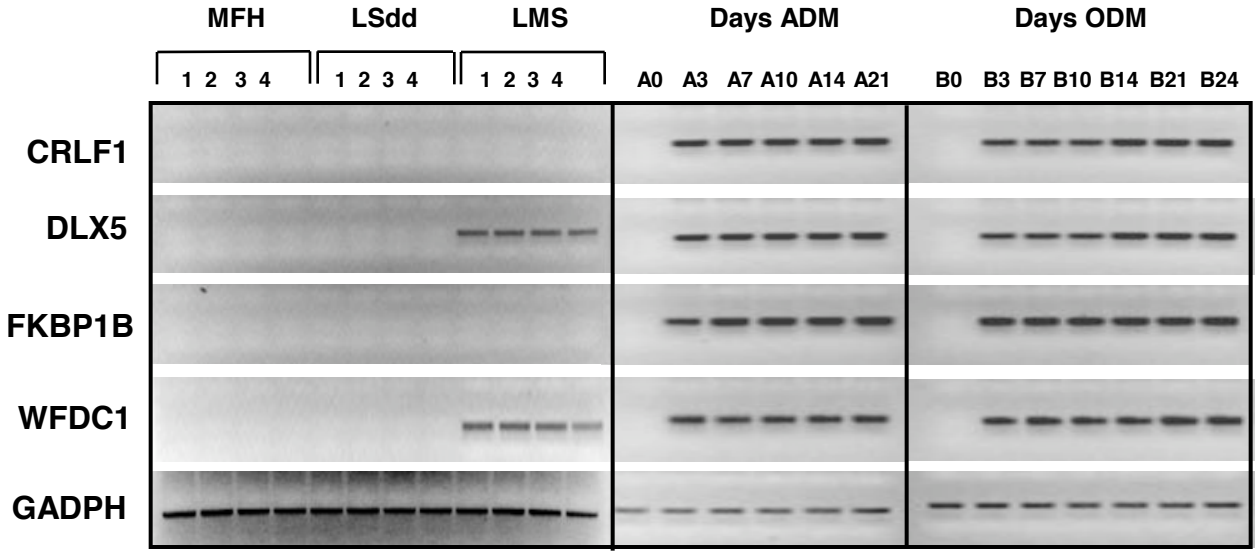

C.

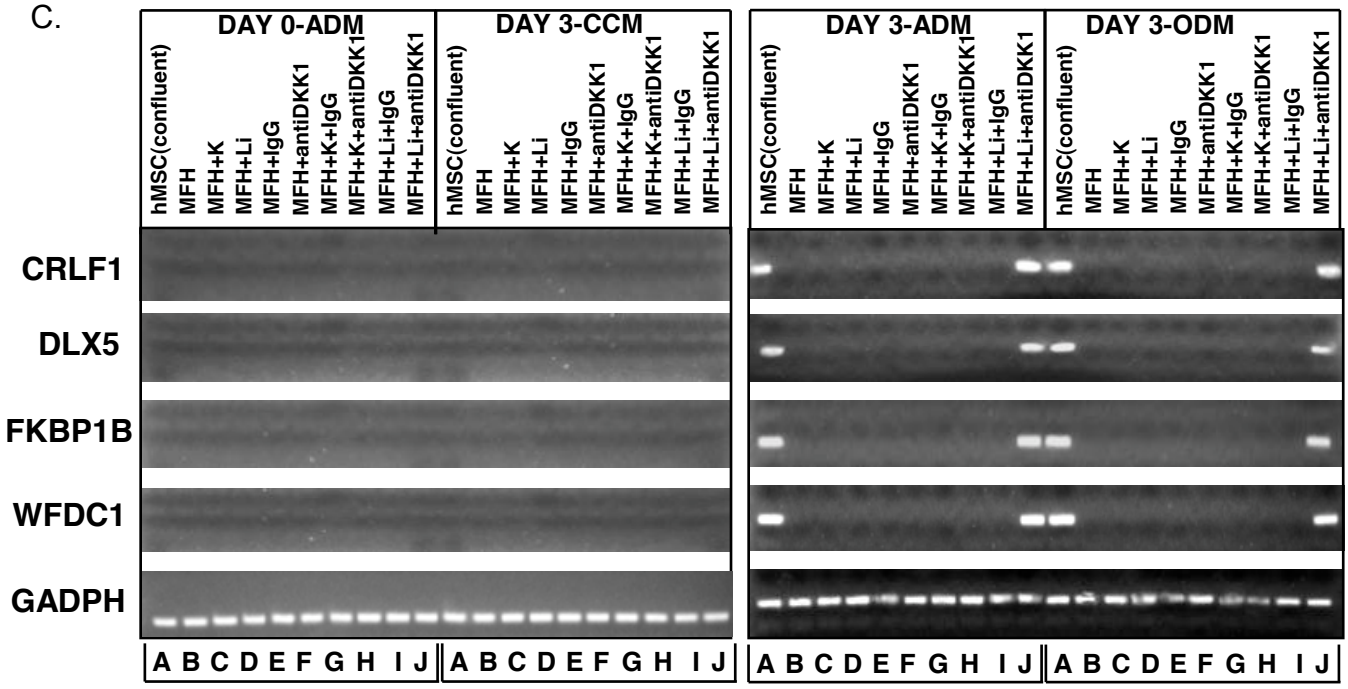

Supp Fig 6:

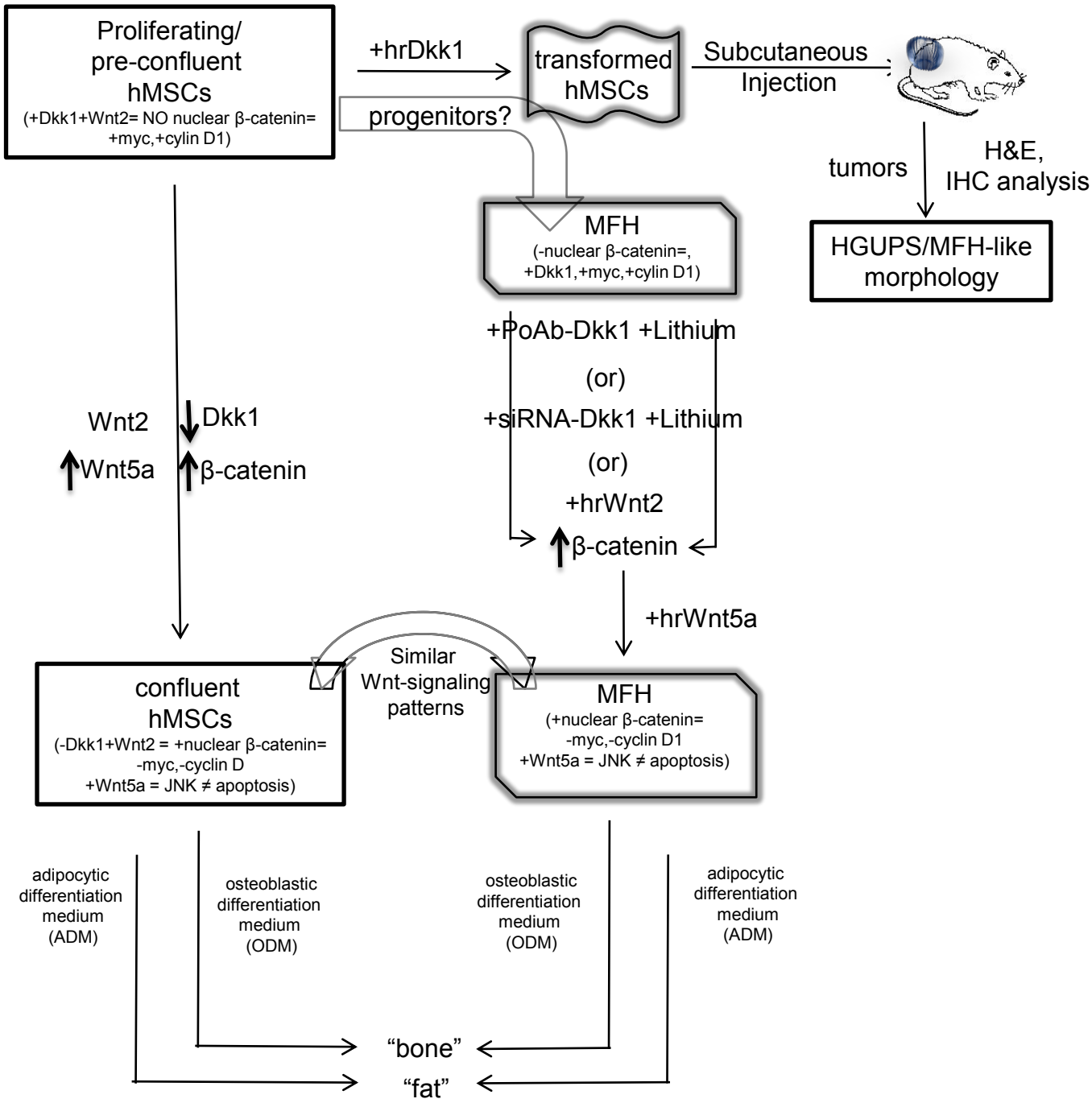
Proliferating/
pre-confluent
hMSCs
(+Dkk1+Wnt2= NO nuclear β-catenin=
+myc,+cylin D1)
+hrDkk1
transformed
hMSCs
Subcutaneous
Injection
progenitors?
tumors
H&E,
IHC analysis
MFH
(-nuclear β-catenin=,
+Dkk1,+myc,+cylin D1)
HGUPS/MFH-like
morphology
+PoAb-Dkk1 +Lithium
(or)
+siRNA-Dkk1 +Lithium
(or)
+hrWnt2
Wnt2
Dkk1
Wnt5a
β-catenin
β-catenin
+hrWnt5a
Similar
Wnt-signaling
patterns
confluent
hMSCs
(-Dkk1+Wnt2 = +nuclear β-catenin=
-myc,-cyclin D
+Wnt5a = JNK ≠ apoptosis)
MFH
(+nuclear β-catenin=
-myc,-cyclin D1
+Wnt5a = JNK ≠ apoptosis)
adipocytic
differentiation
medium
(ADM)
osteoblastic
differentiation
medium
(ODM)
osteoblastic
differentiation
medium
(ODM)
adipocytic
differentiation
medium
(ADM)
"bone"
"fat"